Article

Not peer-reviewed version

State-Selective Differential Cross Sections for Single-Electron Capture in Slow He^+-He Collisions

Shucheng Cui , Kaizhao Lin , Dadi Xing , Ling Liu * , Dongmei Zhao , Dalong Guo , Yong Gao , Shaofeng Zhang , Yong Wu , Chenzhong Dong , Xiaolong Zhu * , Xinwen Ma

Posted Date: 30 July 2025

doi: 10.20944/preprints202507.2549.v1

Keywords: state-selective electron capture; angular differential cross section; two-center close-coupling method; COLTRIMS

 doi:10.20944/preprints202507.2549.v1

Article

State-Selective Differential Cross Sections for Single-Electron Capture in Slow He^+-He Collisions

Shucheng Cui [1,2], Kaizhao Lin [1], Dadi Xing [1], Ling Liu [3,*], Dongmei Zhao [1], Dalong Guo [1,4,5], Yong Gao [1,4,5], Shaofeng Zhang [1,4,5], Yong Wu [3], Chenzhong Dong [2], Xiaolong Zhu [1,4,5,*] and X. Ma [1,4,5]

1 Institute of Modern Physics, Chinese Academy of Sciences, Lanzhou 730000, China
2 College of Physics and Electronic Engineering, Northwest Normal University, Lanzhou 730070, China
3 Key Laboratory of Computational Physics, Institute of Applied Physics and Computational Mathematics, Beijing 100088, China
4 University of Chinese Academy of Sciences, Beijing 100049, China
5 State Key Laboratory of Heavy Ion Science and Technology, Institute of Modern Physics, Chinese Academy of Sciences, Lanzhou 730000, China
* Correspondence: liu_ling@iapcm.ac.cn (L.L.); zhuxiaolong@impcas.ac.cn (X.Z.)

Abstract

A combined experimental and theoretical study is carried out on the single-electron capture process in He^+-He collisions at energies ranging from 0.5 to 5 keV/u. Using cold target recoil ion momentum spectroscopy, we obtain state-selective cross sections and angular differential cross sections. Within the entire studied energy range, the dominant channel is the electron captured into the ground-state, and the relative contribution of the dominant channel shows a decreasing trend with increasing energy. The angular differential cross sections of ground-state capture exhibit obvious oscillatory structures. To understand the oscillatory structures of the differential cross sections, we also performed theoretical calculations using the two-center atomic orbital close-coupling method, which well reproduced the oscillatory structures. The results indicate that these structures are strongly correlated to the oscillatory structures of the impact parameter dependence of electron probability.

Keywords: state-selective electron capture; angular differential cross section; two-center close-coupling method; COLTRIMS

1. Introduction

Charge exchange is not only a fundamental process in atomic physics, but also possesses extensive applications in fields such as astrophysics and fusion plasma physics. In terms of applications, astrophysical studies have shown that the soft X-rays detected from comets can be attributed to the charge exchange processes between solar wind ions and the cometary atmosphere [1–6]. The collision between He^+ and He atoms, as a typical ion-atom interaction system involving three electrons, has been the focus of extensive experimental and theoretical research. This is because it can exhibit the main inelastic reactions (such as electron capture, excitation, ionization, etc.) in ion-atom collisions [7–11]. This collision system has important applications in astrophysics (such as the interaction between the solar wind and planetary atmospheres) and laboratory plasmas (such as the diagnosis of tokamak fusion devices), and its cross-section data are key bases for modeling radiation processes and plasma evolution [12,13].

Early studies were predominantly focused on the measurement of total cross sections. For example, Hegerberg *et al*. measured the total cross section for symmetric charge transfer in He^+-He collisions within the energy range of 1–10 keV [14], and DuBois reported the total cross sections for single electron capture in the range of 3–500 keV [15]. However, they offered only limited information regarding detailed reaction dynamics, which is included in differential cross sections such as angular distributions

 doi:10.20944/preprints202507.2549.v1

and state-selective cross sections. With the advancement of experimental techniques, the application of high-resolution methods especially Cold Target Recoil Ion Momentum Spectroscopy (COLTRIMS) has made it possible to measure state-selective differential cross sections and angular differential cross sections, providing a powerful tool for studying dynamics of ion-atom collisions [16,17].

On the theoretical perspective, early coupled-channel calculations such as the three-electron model proposed by Sural *et al*. considered only a limited number of channels (6 channels) and neglected momentum transfer phases, making it difficult to describe complex many-body interactions [18]. Subsequently, extended models, e.g., the 128-channel calculation by Hildenbrand *et al*. improved computational accuracy but retained limitations, as they have not accounted for the coupling between *s*- and *p*-states [19]. In recent years, the application of methods such as the two-center atomic orbital close-coupling (TC-AOCC) and four-body continuum distorted-wave (CDW-4B) has significantly enhanced the ability to describe state-selective cross sections and angular distributions [20,21]. However, despite numerous studies, state-selective differential cross-section data in the low-energy region remain scarce, and different theoretical models show significant discrepancies in prediction of angular distributions [20]. For instance, the classical trajectory Monte Carlo (CTMC) method has limitations in describing quantum effects in the low-energy region [22,23], while quantum mechanical methods [24], although more accurate, incur high computational costs.

Since the angular differential cross section contains more abundant collision information, it can effectively verify the accuracy of the theoretical models for electron capture processes. One of the characteristics of He^+-He collisions lies in the unique dynamic behaviors induced by their symmetry. Specifically, due to the resonance properties, the ground-state transfer process dominates in the low-energy region, and its angular differential cross section often exhibits oscillatory structures, which makes this collision system an ideal object for testing theoretical models [7,8,10]. Using COLTRIMS setup, this study systematically measured state-selective single-electron capture in the 0.5-5 keV/u He^+-He collision system. Fully differential cross sections for the reaction process are obtained. Obvious oscillatory structures are observed in the angular differential cross sections of the ground-state capture ($1s-1s$) process. Within the measured energy range, the TCAOCC theoretical method well explained these oscillations [20], but the Fraunhofer diffraction theory only shows good agreement at small scattering angles. In addition, our research is compared with the experimental data and theoretical results of Gao et al. [25], and the two studies show good consistency.

2. Experimental Setup

This experiment was conducted on the EBIS platform of the Institute of Modern Physics, Chinese Academy of Sciences as depicted in Figure 1. Detailed information have been provided elsewhere, [26–31]. Briefly, helium is introduced into the EBIS to generate helium ions with varying charge states. These ions are then extracted and sorted by a charge state analyzer to isolate the He^+ ion beam essential for the experiment. Subsequently, the ions are adjusted to the requisite energy for the experiment, passing through a two-dimensional beam-limiting diaphragm and entering a target chamber to collide perpendicularly with the supersonic He target located at the central axis of the Time-of-Flight (TOF) spectrometer. Recoil target ions produced from these collisions are extracted by a uniform electric field oriented perpendicular to both the beam and target directions. They are then detected by a two-dimensional, position-sensitive microchannel plate detector. Post-reaction, scattered projectile ions with various charge states are analyzed by an electrostatic analyzer downstream of the reaction point. Projectiles with reduced charge states are identified by another position-sensitive detector positioned behind the beam, while unreacted projectiles are collected by the Faraday Cup. The TOF spectrometer comprises an acceleration region and a drift region, used to measure the TOF of recoil ions. The experiment utilizes a dual coincidence measurement technique between scattered ions and recoil ions, coupled with an event recording mode measurement. Through analysis of the two-dimensional correlation spectrum between ion positions on the scattering detector and the TOF of the recoil ions, identification of reaction channels like single-electron capture and multiple-electron

 doi:10.20944/preprints202507.2549.v1

capture becomes feasible. For specific reaction channels, analyzing the recoil ion positions on the recoil detector and measuring their time of flight enables the reconstruction of the three-dimensional momentum of the recoil ions.

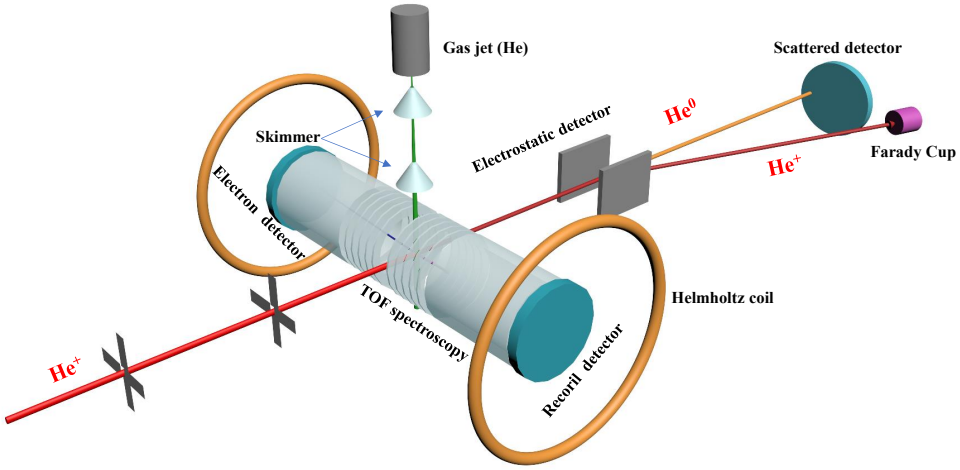

Figure 1. The experimental scheme of COLTRIMS.

Illustrated in Figure 1, the momentum measured along the beam's current direction defines the longitudinal momentum of the recoil ion (P_{long}), while the momentum perpendicular to the beam's direction defines the transverse momentum of the recoil ion (P_{trans}). The fundamental principle of COLTRIMS relies on establishing a relationship between the recoil-ion momentum and two crucial parameters: the Q value representing the binding energy change before and after the collision, and the scattering angle θ of the projectile ion. [16,17] This capture process can be conceptually viewed as an inelastic two-body collision in terms of kinetics. Hence, adhering to the conservation laws of energy and momentum, a simple relation can be derived for small scattering angles:

$$P_{long} = -\frac{Q}{v_o} - \frac{n}{2} \cdot v_o \tag{1}$$

$$\theta = \frac{P_{trans}}{P_o} \tag{2}$$

Here, Q encapsulates details regarding the alteration in binding energy, offering insights into the state populated on the projectile due to the capture process. The variables v_o, n, P_o, and θ denote the projectile velocity, the number of electrons captured by the projectile, the initial momentum of the projectile ion, and the scattering angle of the projectile ion, respectively. It is important to note that all quantities in the equations above are presented in atomic units.

3. Theoretical Method

3.1. Integrated Cross Sections

The application of TC-AOCC method to ion-atom collision system requires determination of the single-center electronic state. The total wave function of the system can be expanded in terms of the electronic states which are centered on the target and projectile, respectively. Inserting the total wave function into the time-dependent Schrödinger equation, one can obtain the coupled equations of the scattering amplitudes [32]. To determine the bound electronic state with Debye–Hückel potential on either of the two centers, Liu et al. used the variational method with even-tempered trial functions by taking the trial functions in the form [33–35]

$$\begin{aligned} \chi_{klm}(\vec{r}) &= N_l(\xi_k) r^l \mathrm{e}^{-\xi_k r} Y_{lm}(\hat{\vec{r}}), \\ \xi_k &= \alpha\beta^k, k = 1, 2, ..., N \end{aligned} \tag{3}$$

 doi:10.20944/preprints202507.2549.v1

where $N_l(\xi_k)$ is a normalization constant, $Y_{lm}(\vec{r})$ are the spherical harmonics and α and β are variational parameters. The atomic states $\phi_{nlm}(\vec{r})$ are then obtained linear combination.

$$\phi_{nlm}(\vec{r}) = \sum_k c_{nk}\chi_{klm}(\vec{r}), \tag{4}$$

where the expansion coefficients c_{nk} are determined by diagonalization of single-centre Hamiltonian. This diagonalization yields the energies $E_{nl}(\alpha)$ of atomic states.

Within the semiclassical approximation, the electron wave function of the He^++He($1s^2$) collision system $\Psi(\vec{r},t)$ satisfies the equation [20]

$$\left(H - i\frac{\partial}{\partial t}\right)\Psi(\vec{r},t) = 0, \tag{5}$$

where

$$H = -\frac{1}{2}\nabla_r^2 + V_A(r_A) + V_B(r_B), \tag{6}$$

and $V_B(r_B)$ are the interactions of the active electron with the projectile (He^+) and target (He) ion core, respectively. The relative motion of the nuclei is described classically by a rectilinear trajectory with a constant velocity v ($(R(t) = \vec{b} + \vec{v}t$, b being the impact parameter). The time-dependent two-center electron wave function is expanded as

$$\Psi(\vec{r},t) = \sum_i a_i(t)\phi_i^A(\vec{r},t) + \sum_j b_j(t)\phi_j^B(\vec{r},t), \tag{7}$$

where $\phi_i^A(\vec{r},t)$ and $\phi_j^B(\vec{r},t)$ are traveling (i.e. containing plane-wave electron translational factors) atomic orbitals centered on the target (A) and the projectile (B). Substituting these into Eq. (5), one obtains the system of coupled equations for the amplitudes $a_i(t)$ and $b_j(t)$ [32],

$$\mathrm{i}(\dot{A} + S\dot{B}) = HA + KB, \tag{8a}$$
$$\mathrm{i}(\dot{B} + S^\dagger\dot{A}) = \bar{K}A + \bar{H}B. \tag{8b}$$

where A and B are vectors representing the amplitudes a_i ($i = 1, 2, ..., N_A$) and b_j ($j = 1, 2, ..., N_B$), respectively. S is the overlap matrix ($S^\dagger$ is its transposed form), H and $\overline{H}$ are direct coupling matrices and K and $\overline{K}$ are the electron-exchange matrices. Equations (8) are solved under the initial conditions

$$a_i(-\infty) = \delta_{1i}, b_j(-\infty) = 0. \tag{9}$$

After solving the system of coupled Eq. (6), the cross section for $1 \to j$ electron capture transition is calculated as

$$\sigma_{cx,j} = 2\pi\int_0^\infty |b_j(+\infty)|^2 b db, \tag{10}$$

The sum of $\sigma_{cx,j}$ over j gives the corresponding total electron capture cross section.

3.2. Differential Cross Sections

The angular-differential cross sections for an inelastic transition from the initial state i to a final state j can be written as

$$\frac{\mathrm{d}\sigma_{ji}}{\mathrm{d}\theta} = 2\pi\sin\theta|A_{ji}|^2, \tag{11}$$

where A_{ji} is the scattering amplitude at a given angle θ. In the eikonal approximation the scattering amplitude is given by

 doi:10.20944/preprints202507.2549.v1

$$A_{ji}(\theta = \mu\nu(-i)^{|m_j-m_i|+1} \int_0^{+\infty} bF(b)\mathrm{d}bJ_{|m_j-m_i|} \times (2b\mu\nu \sin\frac{\theta}{2}), \tag{12}$$

$$F(b) = C_{ji}(b, +\infty)\mathrm{e}^{2(i/\nu)Z_T Z_P \ln b}, \tag{13}$$

where μ is the reduced mass, ν is the relative collision velocity, and $m_j(m_i)$ is the magnetic quantum number of the final (initial) state. The function $J_|m_j - m_i|$ is the Bessel function of the first kind and C_{ji} is the semiclassical transition amplitude for a given impact parameter b. For the considered electron capture process, in the notation of the preceding subsection, $C_{ji} = b_{ij} = b_j(i = 1)$ The factor $\mathrm{e}^{2(i/\nu)Z_T Z_P \ln b}$ is the eikonal phase, Z_T and Z_P being the projectile and target ion-core effective charges, respectively. It is to be noted that the eikonal approximation is valid for small scattering angles (i.e. at collision energies significantly higher than the interaction energy).

4. Results and Discussion

4.1. State-Selective Electron-Capture Process

The longitudinal recoil ion momentum distributions are shown in Figure 2 and the relative cross sections are listed in Table 1. The absolute scale of momentum was calibrated using the well-defined single electron capture process in He^+-He collisions. Different peaks correspond to different final capture states (where n represents the principal quantum number of the captured electron), with the recoil ions being in the ground state. Within the measured energy range, the experimental results indicate that the process of single electron capture into the ground state ($n = 1$) of the projectile is dominant, which is consistent with the consideration of "energy matching". This is a common feature of symmetric ion-atom charge transfer processes, as the ground state transfer in He^+-He collisions is a resonant charge transfer process with a binding energy difference of 0 before and after the reaction. With the increase of projectile energy, in addition to the dominant reaction channel, contributions from excited state transfer (i.e., target electrons captured into states with $n \geq 2$) can be identified, and the relative contribution of this process increases with increasing energy.

Table 1. Relative cross sections (%) of the He^+-He single-electron capture process as a function of collision energy.

E (keV/u)	n = 1	n ≥ 2
0.5	100	
1.25	99.13 ± 0.66	0.87 ± 0.45
2.5	97.75 ± 0.51	2.25 ± 0.33
3.75	97.32 ± 0.68	2.68 ± 0.43
5	96.89 ± 0.42	3.11 ± 0.27

4.2. Angular Differential Cross Sections

In Figure 3, we present the projectile angular distributions of ground-state transfer in the single-electron capture process of He^+-He collisions at energies ranging from 0.25 keV/u to 5 keV/u. The blue solid dots in the figure represent experimental values, the red solid line represents the theoretical calculation results using the TC-AOCC method [20], and the black solid line represents the theoretical calculation results of Fraunhofer-type diffraction [36–38]. In the figure, R is the maximum collision parameter calculated (equivalent to the Fraunhofer diffraction aperture radius). Within the entire studied energy range, the angular differential cross sections of ground-state capture exhibit obvious oscillatory structures. In the past, various mechanisms have been proposed to explain the oscillatory structures observed in angular differential cross sections, such as the interference between gerade and ungerade scattering amplitudes in the quasi-molecular description [25], dynamic effects caused by projectile-electron scattering [39], and diffraction phenomena of matter waves on atoms [38,40]. This explanation for the oscillatory structures in the angular differential cross sections of elastic and

 doi:10.20944/preprints202507.2549.v1

resonant electron capture processes in low-energy collisions of all ion-atom nuclear-symmetric collision systems is widely accepted.

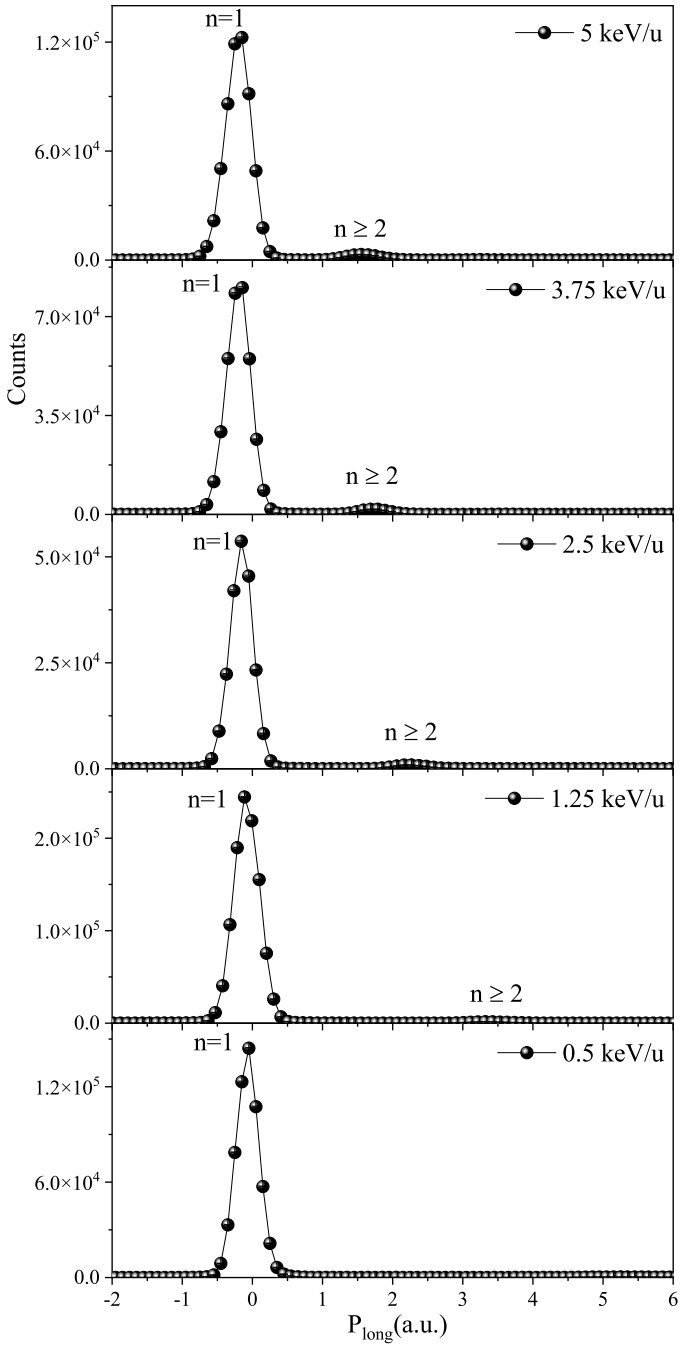

Figure 2. Longitudinal recoil ion momentum for single capture in He^{+}-He collisions at 0.5∼5 keV/u projectile energy.

It can be observed in Figure 3 that within the energy range of this study, the calculation results of the Fraunhofer diffraction theory agree well with the experimental results only at the first maximum; the degree of agreement between the first minimum, the second maximum and the experimental results gradually improves as the collision energy increases. Within this energy range, the Fraunhofer diffraction theory shows an obvious energy dependence and cannot describe the situation of large scattering angles. This characteristic has also been confirmed in the study by Guo et al. [7]. In the study by Gao et al. [10], there was also a deviation between the experimental value and the second minimum, which they attributed to the limitations of the Fraunhofer-type model: first, the interaction region where electron transfer occurs is not an ideal circular aperture; second, at larger scattering

 doi:10.20944/preprints202507.2549.v1

angles, the contribution of hard (small impact parameter) collisions becomes dominant, and there exists a significant internuclear repulsive interaction, which will mask the diffraction pattern.

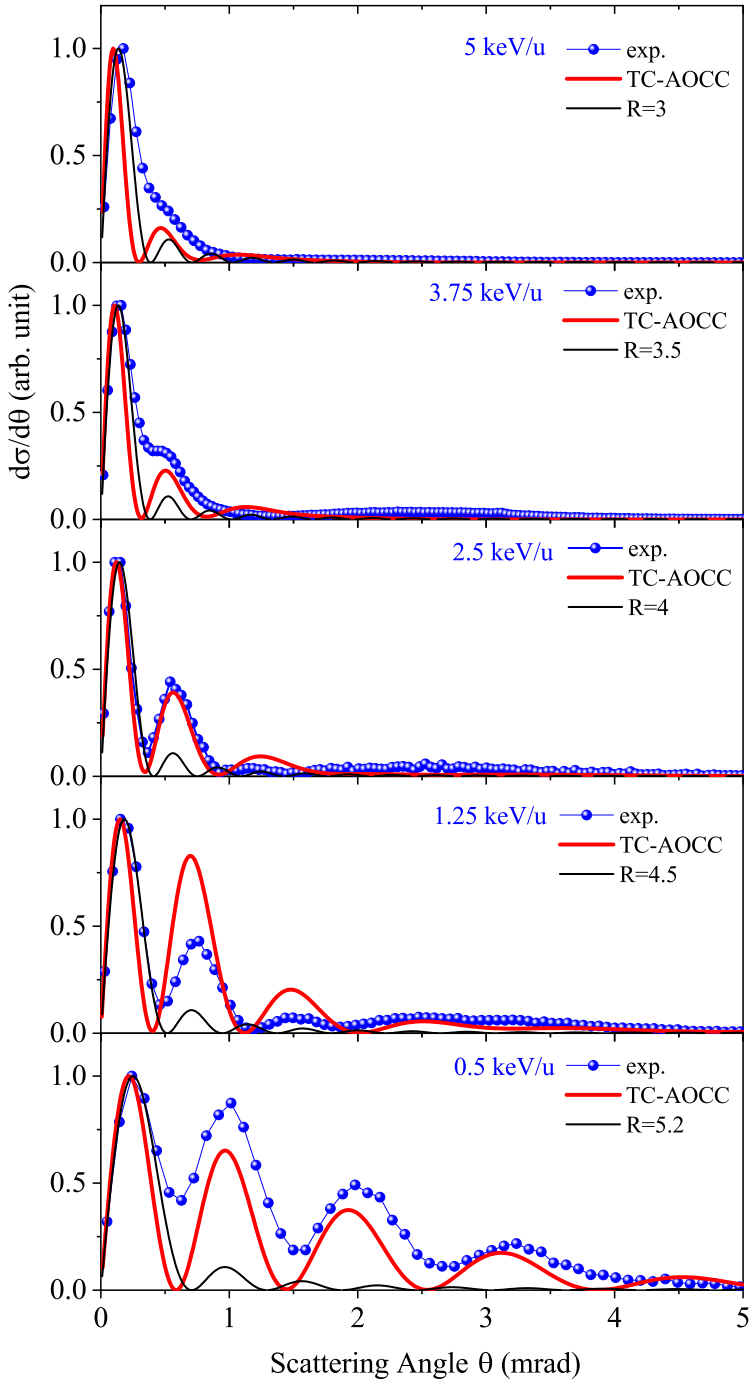

Figure 3. Angular differential cross sections for single electron capture into the ground state ($n = 1$) of projectile He^+ at collision energies from 0.5 keV/u to 5 keV/u. The data are normalized to the maximum of the differential cross section.

In Figure 3, we also present the angular-differential cross sections calculated by the TC-AOCC (Two-Center Atomic Orbital Close-Coupling) method and compare them with the experimental measurement data at the same collision energy. Within the energy range of this study, both the experimental results and the TC-AOCC theoretical results exhibit rich irregular oscillatory structures within the selected angular range. Specifically, for the collision energy E = 0.5 keV/u, the TC-AOCC results agree well with the experimental data when the scattering angle is less than 1.5 mrad; for E = 1.25 keV/u, 2.5 keV/u, 3.75 keV/u, and 5 keV/u, the TC-AOCC results show good agreement with the

 doi:10.20944/preprints202507.2549.v1

experimental data for scattering angles less than 1 mrad. For larger scattering angles, the TC-AOCC results underestimate the cross sections.

Within this energy range, the TC-AOCC calculations also have a good ability to predict the positions of the cross section maxima and minima (especially when $\theta < 2$ mrad). In the angular range of $\theta < 1$ mrad, the calculated oscillation maxima are also in good agreement with the experimental results, but for larger deflection angles, the calculated values tend to be smaller, which is consistent with the research results of Zhao et al. [20]. Compared with the Fraunhofer diffraction theory, the TC-AOCC theory is more suitable for calculating angular-differential cross sections at lower collision energies.

Figure 4 shows the calculated differential cross sections for He^+-He collisions at an energy of 1.25 keV/u, as well as the experimental and theoretical results of Gao et al. [25]. For easier comparison with the experimental data of Gao et al., we adjusted the second maximum of our own experimental data to correspond to the position of the second maximum reported in the study by Gao et al. At this collision energy, our experimental results, along with the experimental and theoretical results of Gao et al., all exhibit rich irregular oscillatory structures within the selected angular range. Among them, the structure of our experimental results at the minima is clearer, which indicates that the resolution of this experiment is higher than that of Gao et al.'s experiment. It can be seen from the figure that our experimental data are in good agreement with the experimental and theoretical results of Gao et al. over the entire studied angular range. In addition, the TC-AOCC calculation results at the energy of 1.25 keV/u and the research results of Gao et al. have been presented in the article by Zhao et al. [20].

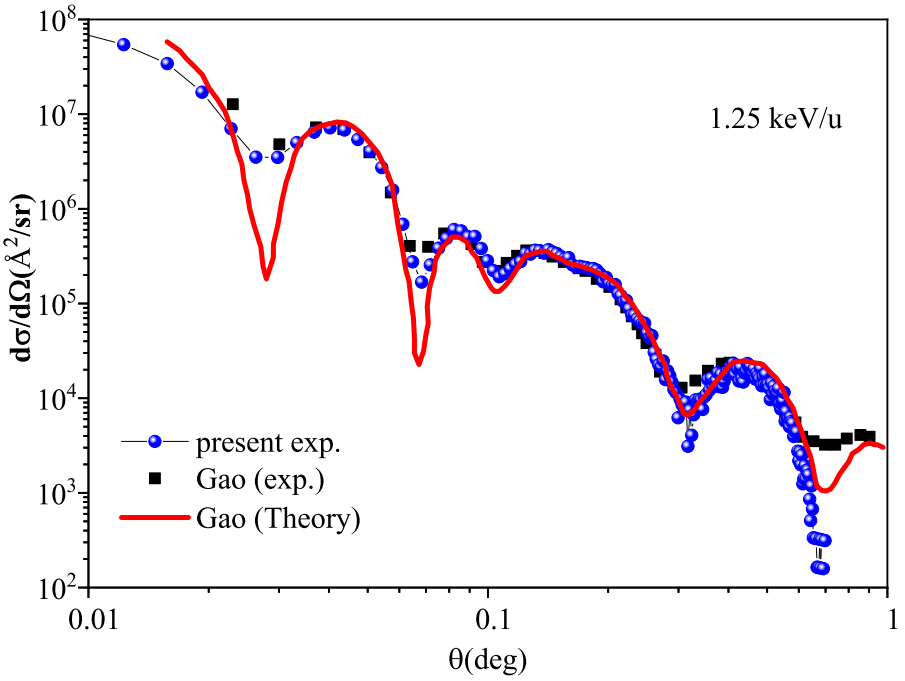

Figure 4. Differential cross section for single electron capture in He^+-He collisions at projectile energies of 1.25 keV/u. The blue solid dots represent our experimental results, the black solid squares represent the experimental values in Gao et al.'s study [25], and the red solid squares represent the quantum–mechanical calculations in Gao et al. [25].

5. Conclusions

In this work, we conducted a combined experimental and theoretical investigation on the single-electron capture process in He^+-He collisions within the energy range of 0.5–5 keV/u. Using the cold target recoil ion momentum spectroscopy (COLTRIMS) technique, we successfully obtained state-selective cross sections and angular differential cross sections for the collision process. Experimental results show that the ground-state resonant transfer ($1s \rightarrow 1s$) is the dominant channel throughout the studied energy range, which is a typical feature of symmetric ion-atom charge transfer reactions. With

 doi:10.20944/preprints202507.2549.v1

the increase of collision energy, the relative contribution of excited-state transfer channels (electrons captured to $n \geq 2$ states) gradually increases, reflecting the evolution of collision dynamics from resonant to non-resonant mechanisms.

The angular differential cross sections of ground-state capture exhibit obvious oscillatory structures, which are closely related to the quantum interference effect in the collision process. Theoretical calculations based on the two-center atomic orbital close-coupling (TC-AOCC) method well reproduce the oscillatory characteristics of the angular differential cross sections, especially in the small scattering angle range ($\theta < 1$ mrad). The TC-AOCC results not only accurately predict the positions of the cross section maxima and minima but also effectively describe the trend of the cross sections with collision energy, confirming that the oscillatory structures originate from the correlation between the impact parameter dependence of electron capture probability and the matter wave diffraction of the projectile. A comparison with the Fraunhofer diffraction model shows that although the latter can explain the first maximum of the angular differential cross section, it has limitations in describing the oscillatory structures at larger angles.

Overall, this work provides reliable experimental data for the single-electron capture process in He^+-He collisions at low energies and verifies the applicability of the TC-AOCC method in describing such collision systems. The results deepen the understanding of the microscopic mechanisms of ion-atom charge transfer, especially the quantum interference and diffraction effects in low-energy collisions, and can provide important reference for related studies in astrophysics and plasma physics.

Author Contributions: Conceptualization, experiment, data analysis, writing—review and editing, X.Z.; writing—original draft preparation, S.C., K.L. D.X., L.L. and X.Z.; Theoretical calculations, L.L. and Y.W. All authors have read and agreed to the published version of the manuscript.

Funding: This research was funded by the National Key Research and Development Program of China under Grant No. 2022YFA1602500 and the Natural Science Foundation of Gansu Province, China under Grant No. 25JRRA461.

Data Availability Statement: All data needed to evaluate the conclusions in this work are present in the paper. Additional raw data are available from the corresponding authors upon reasonable request.

Acknowledgments: Many thanks to the engineers responsible for the operation of the IMP EBIS-A facility.

Conflicts of Interest: The authors declare no conflicts of interest.

References

1. Lisse, C.M.; Dennerl, K.; Englhauser, J.; Harden, M.; Marshall, F.E.; Mumma, M.J.; Petre, R.; Pye, J.P.; Ricketts, M.J.; Schmitt, J.; et al. Discovery of X-ray and Extreme Ultraviolet Emission from Comet C/Hyakutake 1996 B2. *Science* **1996**, *274*, 205–209. https://doi.org/10.1126/science.274.5285.205.
2. Cravens, T.E. Comet Hyakutake X-ray source: Charge transfer of solar wind heavy ions. *Geophysical Research Letters* **1997**, *24*, 105–108. https://doi.org/10.1029/96GL03780.
3. Cravens, T.E. X-ray Emission from Comets. *Science* **2002**, *296*, 1042–1045. https://doi.org/10.1126/science.1070001.
4. Krasnopolsky, V.A.; Mumma, M.J. Spectroscopy of Comet Hyakutake at 80-700 Å: First Detection of Solar Wind Charge Transfer Emissions. *The Astrophysical Journal* **2001**, *549*, 629. https://doi.org/10.1086/319064.
5. Beiersdorfer, P.; Boyce, K.R.; Brown, G.V.; Chen, H.; Kahn, S.M.; Kelley, R.L.; May, M.; Olson, R.E.; Porter, F.S.; Stahle, C.K.; et al. Laboratory simulation of charge exchange-produced X-ray emission from comets. *Science* **2003**, *300*, 1558–1559. https://doi.org/10.1126/science.1084373.
6. Krasnopolsky, V.A.; Greenwood, J.B.; Stancil, P.C. X-ray and extreme ultraviolet emissions from comets. *Space science reviews* **2004**, *113*, 271–373. https://doi.org/10.1023/B:SPAC.0000046754.75560.80.
7. Guo, D.L.; Ma, X.; Zhang, R.T.; Zhang, S.F.; Zhu, X.L.; Feng, W.T.; Gao, Y.; Hai, B.; Zhang, M.; Wang, H.B.; et al. State-selective electron capture in 30- and 100-keV $He^+ + He$ collisions. *Phys. Rev. A* **2017**, *95*, 012707. https://doi.org/10.1103/PhysRevA.95.012707.

 doi:10.20944/preprints202507.2549.v1

8. Schöffler, M.S.; Titze, J.; Schmidt, L.P.H.; Jahnke, T.; Neumann, N.; Jagutzki, O.; Schmidt-Böcking, H.; Dörner, R.; Mančev, I. State-selective differential cross sections for single and double electron capture in $He^{+,2+}$-He and *p*-He collisions. *Phys. Rev. A* **2009**, *79*, 064701. https://doi.org/10.1103/PhysRevA.79.064701.
9. Baxter, M.; Kirchner, T.; Engel, E. Time-dependent spin-density-functional-theory description of He^+-He collisions. *Phys. Rev. A* **2017**, *96*, 032708. https://doi.org/10.1103/PhysRevA.96.032708.
10. Gao, J.W.; Wu, Y.; Wang, J.G.; Sisourat, N.; Dubois, A. State-selective electron transfer in $\mathbf{He^+ + He}$ collisions at intermediate energies. *Phys. Rev. A* **2018**, *97*, 052709. https://doi.org/10.1103/PhysRevA.97.052709.
11. Mančev, I. Four-body continuum-distorted-wave model for charge exchange between hydrogenlike projectiles and atoms. *Phys. Rev. A* **2007**, *75*, 052716. https://doi.org/10.1103/PhysRevA.75.052716.
12. Isler, R.C. A Review of Charge-Exchange Spectroscopy and Applications to Fusion Plasmas. *Physica Scripta* **1987**, *35*, 650. https://doi.org/10.1088/0031-8949/35/5/007.
13. Isler, R.C. An overview of charge-exchange spectroscopy as a plasma diagnostic. *Plasma Physics and Controlled Fusion* **1994**, *36*, 171. https://doi.org/10.1088/0741-3335/36/2/001.
14. Hegerberg, R.; Stefansson, T.; Elford, M.T. Measurement of the symmetric charge-exchange cross section in helium and argon in the impact energy range 1-10 keV. *Journal of Physics B: Atomic and Molecular Physics* **1978**, *11*, 133. https://doi.org/10.1088/0022-3700/11/1/017.
15. DuBois, R.D. Multiple ionization in He^+–rare-gas collisions. *Phys. Rev. A* **1989**, *39*, 4440–4450. https://doi.org/10.1103/PhysRevA.39.4440.
16. Ullrich, J.; Moshammer, R.; Dörner, R.; Jagutzki, O.; Mergel, V.; Schmidt-Böcking, H.; Spielberger, L. Recoil-ion momentum spectroscopy. *Journal of Physics B: Atomic, Molecular and Optical Physics* **1997**, *30*, 2917. https://doi.org/10.1088/0953-4075/30/13/006.
17. Dörner, R.; Mergel, V.; Jagutzki, O.; Spielberger, L.; Ullrich, J.; Moshammer, R.; Schmidt-Böcking, H. Cold Target Recoil Ion Momentum Spectroscopy: a 'momentum microscope' to view atomic collision dynamics. *Physics Reports* **2000**, *330*, 95–192. https://doi.org/https://doi.org/10.1016/S0370-1573(99)00109-X.
18. Sural, D.P.; Mukherjee, S.C.; Sil, N.C. Electron Capture and Excitation in He^+-He Collisions. *Phys. Rev.* **1967**, *164*, 156–165. https://doi.org/10.1103/PhysRev.164.156.
19. Hildenbrand, R.; Grun, N.; Scheid, W. Coupled channel calculations with Cartesian Gaussian basis functions for H+He and He^++He reactions. *Journal of Physics B: Atomic, Molecular and Optical Physics* **1995**, *28*, 4781. https://doi.org/10.1088/0953-4075/28/22/010.
20. Zhao, G.P.; Liu, L.; Chang, Z.; Wang, J.G.; Janev, R.K. Total, state-selective and differential cross sections for single electron capture in He^+–He collisions. *Journal of Physics B: Atomic, Molecular and Optical Physics* **2018**, *51*, 085201. https://doi.org/10.1088/1361-6455/aab426.
21. Jana, D.; Purkait, K.; Haque, A.; Mondal, M.; Halder, S.; Purkait, M. State-selective differential and total cross sections for single-electron capture in He^+-He collisions. *Indian Journal of Physics* **2022**, *96*, 4071–4081. https://doi.org/10.1007/s12648-022-02353-9.
22. Mergel, V.; Dörner, R.; Achler, M.; Khayyat, K.; Lencinas, S.; Euler, J.; Jagutzki, O.; Nüttgens, S.; Unverzagt, M.; Spielberger, L.; et al. Intra-atomic Electron-Electron Scattering in *p*-He Collisions (Thomas Process) Investigated by Cold Target Recoil Ion Momentum Spectroscopy. *Phys. Rev. Lett.* **1997**, *79*, 387–390. https://doi.org/10.1103/PhysRevLett.79.387.
23. Moshammer, R.; Ullrich, J.; Kollmus, H.; Schmitt, W.; Unverzagt, M.; Jagutzki, O.; Mergel, V.; Schmidt-Böcking, H.; Mann, R.; Wood, C.J.; et al. Double Ionization of Helium and Neon for Fast Heavy-Ion Impact: Correlated Motion of Electrons from Bound to Continuum States. *Phys. Rev. Lett.* **1996**, *77*, 1242–1245. https://doi.org/10.1103/PhysRevLett.77.1242.
24. Wang, X.X.; Wang, K.; Peng, Y.G.; Liu, C.H.; Liu, L.; Wu, Y.; Liebermann, H.P.; Buenker, R.J.; Qu, Y.Z. Ab Initio Study of Single- and Double-Electron Capture Processes in Collisions of He^{2+} Ions and Ne Atoms. *Chinese Physics Letters* **2021**, *38*, 113401. https://doi.org/10.1088/0256-307X/38/11/113401.
25. Gao, R.S.; Johnson, L.K.; Schafer, D.A.; Newman, J.H.; Smith, K.A.; Stebbings, R.F. Absolute differential cross sections for small-angle He^+-He elastic and charge-transfer scattering at keV energies. *Phys. Rev. A* **1988**, *38*, 2789–2793. https://doi.org/10.1103/PhysRevA.38.2789.
26. Ma, X.; Zhang, R.T.; Zhang, S.F.; Zhu, X.L.; Feng, W.T.; Guo, D.L.; Li, B.; Liu, H.P.; Li, C.Y.; Wang, J.G.; et al. Electron emission from single-electron capture with simultaneous single-ionization reactions in 30-keV/u He^{2+}-on-argon collisions. *Phys. Rev. A* **2011**, *83*, 052707. https://doi.org/10.1103/PhysRevA.83.052707.
27. Zhu, X.; Ma, X.; Li, J.; Schmidt, M.; Feng, W.; Peng, H.; Xu, J.; Zschornack, G.; Liu, H.; Zhang, T.; et al. A compact, flexible low energy experimental platform of highly charged ions for atomic physics experiments.

 doi:10.20944/preprints202507.2549.v1

Nuclear Instruments and Methods in Physics Research Section B: Beam Interactions with Materials and Atoms **2019**, *460*, 224–229. https://doi.org/https://doi.org/10.1016/j.nimb.2018.11.047.

28. Zhu, X.; Cui, S.; Xing, D.; Xu, J.; Najjari, B.; Zhao, D.; Guo, D.; Gao, Y.; Zhang, R.; Su, M.; et al. State-selective charge exchange cross sections in collisions of highly-charged sulfur ions with helium and molecular hydrogen. *Chinese Physics B* **2024**, *33*, 023401. https://doi.org/10.1088/1674-1056/ad0b01.
29. Cui, S.; Xing, D.; Zhu, X.; Su, M.; Gao, Y.; Guo, D.; Zhao, D.; Zhang, S.; Fu, Y.; Ma, X. The n-resolved single-electron capture in slow O^{6+}-Ne collisions. *Chinese Physics B* **2024**, *33*, 073401. https://doi.org/10.1088/1674-1056/ad39d2.
30. Xing, D.; Cui, S.; Wang, X.; Zhang, D.; Zhu, X.; Lin, K.; Gao, Y.; Guo, D.; Zhao, D.; Zhang, S.; et al. State-selective single- and double-electron capture in slow N^{4+}-He collisions. *Phys. Rev. A* **2025**, *112*, 012812. https://doi.org/10.1103/lgyj-yzrk.
31. Li, Z.; Lin, K.; Zhu, X.; Li, Z.; Yuan, H.; Gao, Y.; Guo, D.; Zhao, D.; Zhang, S.; Ma, X. Fragmentation dynamics of nitric oxide induced by low-energy heavy ions. *Chinese Physics B* **2025**, *34*, 053401. https://doi.org/10.1088/1674-1056/adbdc0.
32. Fritsch, W.; Lin, C. The semiclassical close-coupling description of atomic collisions: Recent developments and results. *Physics Reports* **1991**, *202*, 1–97. https://doi.org/https://doi.org/10.1016/0370-1573(91)90008-A.
33. Liu, L.; Wang, J.G.; Janev, R.K. Dynamics of $He^{2+} + H(1s)$ excitation and electron-capture processes in Debye plasmas. *Phys. Rev. A* **2008**, *77*, 032709. https://doi.org/10.1103/PhysRevA.77.032709.
34. Liu, L.; Wang, J.G.; Janev, R.K. Dynamics of $O^{8+} + H$ electron capture in Debye plasmas. *Phys. Rev. A* **2009**, *79*, 052702. https://doi.org/10.1103/PhysRevA.79.052702.
35. Kuang, J.; Lin, C.D. Convergent TCAO close-coupling calculations for electron transfer, excitation and ionization in intermediate keV collisions. *Journal of Physics B: Atomic, Molecular and Optical Physics* **1997**, *30*, 101. https://doi.org/10.1088/0953-4075/30/1/012.
36. van der Poel, M.; Nielsen, C.V.; Gearba, M.A.; Andersen, N. Fraunhofer Diffraction of Atomic Matter Waves: Electron Transfer Studies with a Laser Cooled Target. *Phys. Rev. Lett.* **2001**, *87*, 123201. https://doi.org/10.1103/PhysRevLett.87.123201.
37. van der Poel, M.; Nielsen, C.V.; Rybaltover, M.; Nielsen, S.E.; Machholm, M.; Andersen, N. Atomic scattering in the diffraction limit: electron transfer in keV Li^+–Na(3s, 3p) collisions. *Journal of Physics B: Atomic, Molecular and Optical Physics* **2002**, *35*, 4491. https://doi.org/10.1088/0953-4075/35/21/312.
38. Wang, Q.; Ma, X.; Zhu, X.L.; Zhang, S.F. Observation of atomic-size Fraunhofer-type diffraction for single electron capture in He^{2+} + He collision. *Journal of Physics B: Atomic, Molecular and Optical Physics* **2011**, *45*, 025202. https://doi.org/10.1088/0953-4075/45/2/025202.
39. Horsdal, E.; Jensen, B.; Nielsen, K.O. Critical Angle in Electron Capture. *Phys. Rev. Lett.* **1986**, *57*, 1414–1416. https://doi.org/10.1103/PhysRevLett.57.1414.
40. Knoop, S.; Olson, R.E.; Ott, H.; Hasan, V.G.; Morgenstern, R.; Hoekstra, R. Single ionization and electron capture in He^{2+}+Na collisions. *Journal of Physics B: Atomic, Molecular and Optical Physics* **2005**, *38*, 1987. https://doi.org/10.1088/0953-4075/38/12/013.